

# 2D nanosheet-constructed hybrid nanofillers for polymer nanocomposites with synergistic dispersion and function

Cite as: APL Mater. 7, 080904 (2019); doi: 10.1063/1.5110228

Submitted: 15 May 2019 • Accepted: 31 July 2019 •

Published Online: 20 August 2019



View Online



Export Citation



CrossMark

Ying Liu,<sup>1</sup> Yufeng Wang,<sup>1</sup> Chao Zhang,<sup>1,a)</sup>  and Tianxi Liu<sup>1,2,a)</sup>

## AFFILIATIONS

<sup>1</sup>State Key Laboratory for Modification of Chemical Fibers and Polymer Materials, College of Materials Science and Engineering, Innovation Center for Textile Science and Technology, Donghua University, Shanghai 201620, People's Republic of China

<sup>2</sup>Key Laboratory of Synthetic and Biological Colloids, Ministry of Education, School of Chemical and Material Engineering, Jiangnan University, Wuxi 214122, People's Republic of China

<sup>a)</sup>Authors to whom correspondence should be addressed: [czhang@dhu.edu.cn](mailto:czhang@dhu.edu.cn) and [txliu@fudan.edu.cn](mailto:txliu@fudan.edu.cn). Tel.: +86-21-67874060. Fax: +86-21-67874093.

## ABSTRACT

Polymer nanocomposites (PNCs) are new-emerging multicomponent polymer composites consisting of a polymer matrix and well dispersed nanofillers. Nanofillers can be divided into one-dimensional, two-dimensional (2D), or three-dimensional nanoparticles according to their dimensions. Due to their outstanding physical properties, the achievement of homogeneous dispersion of 2D nanofillers in the polymer matrix plays a decisive role in the fabrication of high-performance and multifunctional PNCs. The construction of 2D nanosheets into hybrid nanofillers provides a new idea for achieving homogeneous dispersion of 2D nanofillers in the polymer matrix. In this review, recent developments on the design strategies and controllable preparation methods of hybrid nanofillers containing 2D nanosheets are summarized. The preparation, structure, and physical properties of PNCs with 2D nanosheet-constructed hybrid nanofillers are discussed in detail. Finally, challenges and future prospects of PNCs with 2D nanosheet-constructed hybrid nanofillers are highlighted.

© 2019 Author(s). All article content, except where otherwise noted, is licensed under a Creative Commons Attribution (CC BY) license (<http://creativecommons.org/licenses/by/4.0/>). <https://doi.org/10.1063/1.5110228>

## I. INTRODUCTION

Polymer nanocomposites (PNCs) are new-emerging polymer composites consisting of a polymer with nanofillers dispersed in the polymer matrix. Compared with conventional polymer composites, the PNCs with an integrated structure and function usually show greatly improved physical properties due to unique structures and excellent properties of nanofillers. According to different dimensions, nanofillers can be divided into one-dimensional (1D), two-dimensional (2D), and three-dimensional (3D) nanofillers. In particular, 2D nanosheets with the features of high surface area, large radius-to-thickness ratio, and superior physical properties are intensively triggering the fast development of high-performance PNCs.<sup>1</sup> 2D nanosheets are easy to agglomerate because of their high surface energy, because of which it is difficult to achieve uniform dispersion in the polymer matrix and thus greatly limits the

application of 2D nanosheets in high-performance PNCs. The fabrication of 2D nanosheet-constructed hybrid nanofillers is beneficial to improve the uniform dispersion of the elementary nanoparticles among hybrid nanofillers in the polymer matrix.<sup>2</sup> Besides, the enhancement of PNCs with single-component nanofillers is somewhat at an unsatisfactory level, and the construction of PNCs with two kinds of nanofillers is beneficial to synergistically improve physical properties of PNCs by combining desirable elementary nanoparticles into hybrid nanofillers according to their various functions.<sup>3</sup>

Figure 1 demonstrates the commonly used 2D nanofillers including clay, graphene, and transition metal dichalcogenides (TMDs) for the construction of hybrid nanofillers in high-performance PNCs. The structural models of montmorillonite (MMT), graphene, and MoS<sub>2</sub> are exhibited in Fig. 1. Single-layered MMT is a type of silicate clay with a configuration of two silica tetrahedral layers and an edge-shared octahedral metal oxide layer,

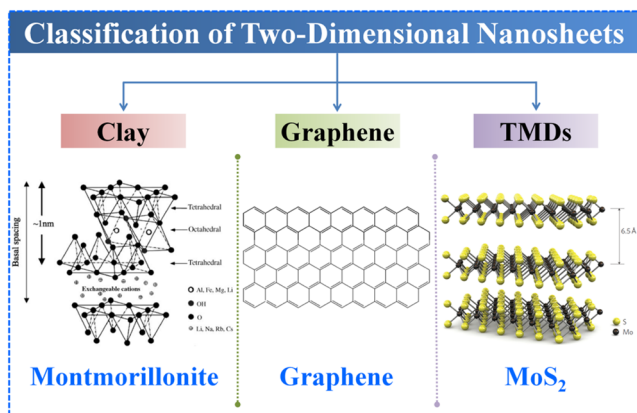


**FIG. 1.** Structural models of commonly used 2D nanosheets such as clay, graphene, and TMDs for fabricating hybrid nanofillers.<sup>4,7,8</sup> Reproduced with permission from S. Sinha Ray and M. Okamoto, *Prog. Polym. Sci.* **28**(11), 1539–1641 (2003). Copyright 2003 Elsevier; Radisavljevic *et al.*, *Nat. Nanotechnol.* **6**(3), 147–150 (2011). Copyright 2011 Springer Nature; and G. Kucinskis, G. Bajars, and J. Kleperis, *J. Power Sources* **240**, 66–79 (2013). Copyright 2013 Elsevier.

which is one of the most common nanofillers with naturally abundant resources.<sup>4</sup> Graphene, a single-atom-thick carbon nanosheet with a planar honeycomb lattice, is a research hotspot in various fields since its discovery. Compared with the MMT, graphene is one kind of nanofillers with extremely low density for fabricating multifunctional PCNs due to its superior mechanical, electrical, and thermal properties.<sup>5</sup> TMDs (such as MoS<sub>2</sub>, MoSe<sub>2</sub>, and WS<sub>2</sub>), a high band gap semiconductor, can significantly improve the mechanical and thermal properties of the polymer matrix without significantly influencing the electrical conductivity of PCNs.<sup>6</sup>

Although the achievement of homogeneous dispersion of functionalized 2D nanofillers within PNCs has been intensely investigated in recent years, there is still a lack of systematic summary on the construction of hybrid nanofillers containing 2D nanofillers for high-performance and multifunctional PNCs. In view of this, the design principles and controllable preparations of hybrid nanofillers containing 2D nanofillers for fabricating PNCs are summarized and discussed. The physical properties of as-fabricated PNCs including the mechanical properties, electrical conductivities, and thermal properties are also discussed. Finally, an outlook in terms of the preparations and applications of hybrid nanofillers for high-performance PNCs is highlighted.

## II. STRATEGIES TO FABRICATE HYBRID NANOFILLERS CONTAINING 2D NANOSHEETS

Hybrid nanofillers constructed of 2D nanofillers with other functional nanofillers (1D, 2D, or 3D nanoparticles) facilitate the fabrication of high-performance and multifunctional PNCs. Figures 2(a)–2(c) illustrate 2D-1D, 2D-2D, and 2D-3D structural models for construction of hybrid nanofillers. Hybrid nanofillers with diverse morphologies have been achieved depending on various shapes, sizes, and surface characteristics of nanofillers and the way they are hybridized. For instance, for the 2D-1D structure, 1D carbon nanotubes (CNTs) are observed to attach to 2D reduced

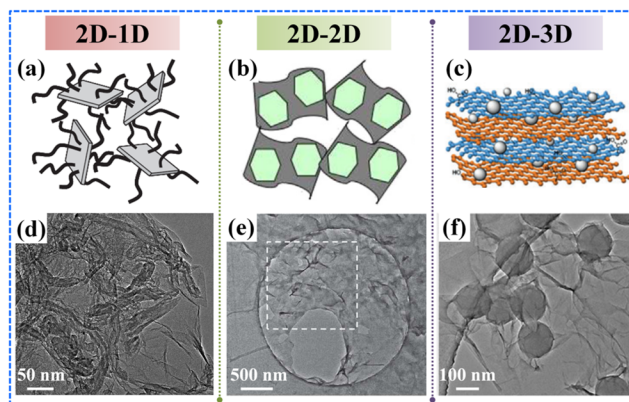


**FIG. 2.** Schematic of (a) 2D-1D, (b) 2D-2D, and (c) 2D-3D structural models for fabricating hybrid nanofillers.<sup>9–11</sup> TEM images of (d) GO/CNT, (e) r-GO/MMT, and (f) r-GO/carbon nanosphere hybrids.<sup>12–14</sup> Reproduced with permission from W. D. Zhang, I. Y. Phang, and T. X. Liu, *Adv. Mater.* **18**(1), 73–77 (2006). Copyright 2006 John Wiley & Sons, Inc.; Wang *et al.*, *ChemPlusChem* **79**(3), 375–381 (2014). Copyright 2014 John Wiley & Sons, Inc.; Zhou *et al.*, *Mater. Chem. Phys.* **178**, 1–5 (2016). Copyright 2016 Elsevier; C. Zhang *et al.*, *J. Mater. Chem.* **22**(6), 2427–2434 (2012). Copyright 2012 The Royal Society of Chemistry; C. Zhang *et al.*, *J. Mater. Chem.* **21**(44), 18011–18017 (2011). Copyright 2011 The Royal Society of Chemistry; and Z. Huang, H. Guo, and C. Zhang, *Compos. Commun.* **12**, 117–122 (2019). Copyright 2009 Elsevier.

graphene oxide (r-GO) to form a unique r-GO/CNT (G-CNT) hybrid [Fig. 2(d)]. For the 2D-2D structure, two kinds of 2D nanosheets are observed to form a laminated structure of r-GO/MMT hybrid [Fig. 2(e)]. The MMT nanosheets are successfully attached on the surface of r-GO nanosheets, which is beneficial to improve the dispersion of MMT in the polymer matrix. For the 2D-3D structure, 3D nanospheres can be effectively hybridized with 2D nanosheets, as observed in representative Transmission Electron Microscope (TEM) image of r-GO/carbon nanosphere hybrid [Fig. 2(f)]. The surface of r-GO nanosheets is covered with narrowly distributed carbon nanospheres with no obvious aggregation. In Secs. II A–II C, recent progress on the design strategies to prepare hybrid nanofillers containing 2D nanosheets of various structural models is presented.

### A. 2D-1D hybrid nanofillers

The combination of 2D and 1D nanofillers illustrates a unique synergistic dispersion to construct a unique 3D nanostructure with homogeneous dispersion of each component within the polymer matrix. Moreover, high surface area, good electrical conductivity, and tailored porosity of PNCs can be further benefited due to the introduction of the unique 2D-1D hybrid nanofillers. CNTs have been widely used as 1D nanofillers with superior reinforcement for PNCs due to their unique properties such as high aspect ratio, high tensile strength, and high conductivity. Various routes toward the preparation of 1D CNT-incorporated hybrid nanofillers have been described in the literature, and the main approaches are based on the solution-processed self-assembly<sup>12,15,16</sup> and *in situ* chemical vapor deposition (CVD) growth strategies.<sup>9,17</sup>

The solution-processed self-assembly is typically driven by interactions including hydrogen bonding, electrostatic adsorption, and van der Waals force between 1D and 2D carbon nanofillers. Traditional stabilizing agents for dispersion of nanofillers are avoidable in this strategy. For instance, Srivastava and co-workers have prepared a multiwalled carbon nanotube (MWCNT)-graphene hybrid via a simple solution-mixing method followed by using the hybrid nanofillers for silicone rubber nanocomposites by solution-casting.<sup>18</sup> The PNCs show the synergistic enhanced performance in tensile strength (110%) and Young's modulus (137%) as well as thermal stability compared to a neat silicone rubber matrix. Graphene oxide (GO) nanosheets contain multiple aromatic regions and hydrophilic oxygen groups, and therefore, pristine CNTs can be well dispersed in water and anchored on the GO sheets through  $\pi$ - $\pi$  stacking interaction, thus forming a GO/CNT hybrid. Conversely, a G-CNT hybrid of r-GO and acid-treated carbon nanotubes (t-CNTs) has been prepared via direct chemical reduction of GO in water in the presence of t-CNTs [Fig. 3(a)]. In this case, the G-CNT hybrid has been solution-casted with poly(vinyl alcohol) (PVA) to form nanocomposites with fine dispersions of both r-GO and t-CNTs [Fig. 3(b)]. With addition of only 0.6 wt. % G-CNT hybrid, the tensile strength and Young's modulus of the PVA nanocomposite were improved by 77% and 65%, respectively.

Although the solution-processed self-assembly is a simple and effective method for fabricating carbon-based 2D-1D hybrid nanofillers, several drawbacks have to be solved, including the following. First, the content of hybrid nanofillers within the PCNs is limited because the hybrid nanofillers will aggregate in solution at a relatively large concentration. Second, the alignments of anisotropic 1D and 2D nanofillers are difficult to achieve via simple solution-casting, which is very conducive to dramatically improving the physical properties of as-obtained PCNs under certain direction.

Third, the solution-processed self-assembly is usually accompanied with environmental damages due to the use of large quantity solvents. Thus, the solution-processed self-assembly toward the preparation of hybrid nanofillers is limited for large-scale manufacturing of PNCs.

The CVD growth method is a cost-efficient way for the commercial production of CNTs.<sup>19</sup> Therefore, *in situ* CVD growth of CNTs on 2D nanofillers is another strategy to form the 2D-1D hybrid nanofillers. During *in situ* CVD process, the vapor-phase carbon sources prefer to deposit on the catalytic site-embedded 2D nanofillers. The diameter, density, and orientation of deposited CNTs can be controlled by tailoring the CVD parameters such as temperature, chamber pressure, carrier gas velocity, catalytic site/source ratio, and source-substrate distance. *In situ* CVD growth of CNTs on 2D MMT nanosheets has been adapted to form the MMT/CNT hybrid, which was then incorporated into the polyamide 6 (PA6) matrix with fine dispersion by melt-compounding [Fig. 3(c)].<sup>9,20</sup> Specifically, the MMT was exfoliated by the intercalation of  $\text{Fe}_2\text{O}_3$  particles between its interlayers by calcination, and then,  $\text{Fe}_2\text{O}_3$  particles will be reduced to Fe catalysts for *in situ* CVD growth of CNTs.

Besides the *in situ* CVD growth of CNTs onto 2D nanosheets, the deposition of 2D nanosheets onto the CNT backbone is practical to obtain a 2D-1D hybrid. Gui and co-workers reported the preparation of a  $\text{MoS}_2$  nanolayer-wrapped CNT hybrid by growing  $\text{MoS}_2$  nanosheets onto CNTs.<sup>21</sup> The as-obtained epoxy nanocomposites reinforced with the  $\text{MoS}_2$ /CNT hybrid show good dispersion and remarkable improvements in mechanical, thermal, and flame retardancy performance.

In addition, 1D nanowires have also been used to construct hybrid nanofillers for PNCs. Compared with 1D CNTs, the microstructure, composition, and surface properties of 1D

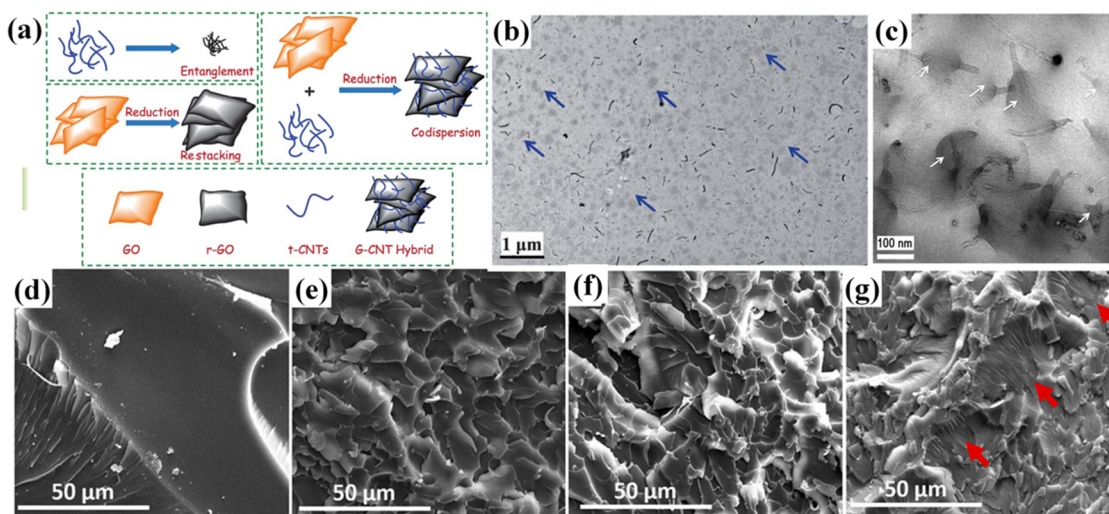


**FIG. 3.** (a) Schematic of synergistic dispersion of the G-CNT hybrid.<sup>12</sup> (b) TEM image of the G-CNT hybrid within the PVA matrix.<sup>12</sup> (c) TEM image of the MMT/CNT hybrid within the PA6 matrix.<sup>20</sup> Fracture-surface SEM images of (d) neat epoxy and its nanocomposites with (e) 1 wt. % of  $\text{MoS}_2$ , (f) h-BN, and (g)  $\text{MoS}_2$ /h-BN hybrid.<sup>28</sup> Reproduced by permission of The Royal Society of Chemistry C. Zhang *et al.*, *J. Mater. Chem.* **22**(6), 2427–2434 (2012). Copyright 2012 The Royal Society of Chemistry. Reproduced with permission from Zhang *et al.*, *J. Phys. Chem. B* **115**(13), 3392–3399 (2011). Copyright 2011 American Chemical Society; Ribeiro *et al.*, *ACS Appl. Mater. Interfaces* **11**(27), 24485–24492 (2019). Copyright 2019 American Chemical Society.

nanowires can be easily tailored at different synthesis conditions. For instance, Yu and co-workers fabricated a GO/xonotlite nanowire (XNW) hybrid via hydrogen bonding interaction, which can be easily penetrated into a polyacrylamide (PAM) hydrogel network.<sup>22</sup> The as-fabricated PAM/GO/XNW hydrogel exhibits a high toughness of  $22 \text{ MJ m}^{-3}$  at a tensile elongation of 2750%, which is 45 times higher than that of neat PAM hydrogel.

## B. 2D-2D hybrid nanofillers

Hybridization of 2D nanosheets with other 2D nanosheets shows a synergistic dispersion and function on the reinforcement of as-obtained PNCs. The combination of each component can be achieved with tailored properties of individual nanofillers, enabling the PNCs for multifunctional applications. Depending on the resultant morphology, 2D-2D hybrid nanofillers include the hybridization of two kinds of 2D nanosheets with similar and totally different sizes, respectively.

Two kinds of 2D nanosheets at comparable sizes will easily self-assemble into a unique ordered hybrid structure. For instance, r-GO nanosheets can be well stabilized in water by the direct reduction of GO sheets in the presence of exfoliated MMT.<sup>13</sup> In this case, laminar r-GO and MMT nanosheets show similar sizes with a dimension of several micrometers. Two types of interfacial interactions between r-GO and MMT nanosheets include hydrogen-bonding interaction and electrostatic interaction linked with sodium ions, contributing to the formation of a water-dispersible r-GO/MMT hybrid. Upon filtration, the 2D r-GO and MMT nanosheets self-assemble to form a hybrid film with a priority orientation. Combining the advantage of these 2D nanosheets, the obtained hybrid films own excellent flexibility, electrical conductivity, and fire resistance. Huang and co-workers grafted modified nanoclay onto the surface of r-GO nanosheets and then incorporated the hybrid nanofillers into the epoxy matrix.<sup>23</sup> In this case, r-GO sheets are covered on decorated nanoclay. The epoxy nanocomposite shows improved thermomechanical and flame retardant properties due to synergistic dispersion of hybrid nanofillers.

MoS<sub>2</sub> has received special attention because of its unique features such as high thermal/chemical stability, excellent mechanical strength, and high thermal conductivity, which shows a potential for wide-range applications in transistors, photodetectors, solar cells, gas sensors, etc.<sup>24–27</sup> Ajayan and co-workers employed a MoS<sub>2</sub>/hexagonal boron nitride (h-BN) hybrid nanofiller to improve the physical properties of epoxy nanocomposites.<sup>28</sup> The MoS<sub>2</sub>/h-BN hybrid nanofiller was prepared via ultrasonic exfoliation together with roll milling. The unique hybrid with two 2D nanosheets imparts a synergistic reinforcement to epoxy by causing 95% increase in tensile strength, 60% in ultimate strain, 58% in Young's modulus, and 203% in thermal conductivity. Figures 3(d)–3(g) show the Scanning Electron Microscope (SEM) images of fractured surfaces of neat epoxy and its nanocomposites containing 1.0 wt. % of MoS<sub>2</sub>, h-BN, and MoS<sub>2</sub>/h-BN hybrid, respectively. Neat epoxy shows a smooth surface, while the nanocomposite shows a roughness with different profiles. The MoS<sub>2</sub>/h-BN hybrid nanofillers work as anchoring points for epoxy chains [highlighted in Fig. 3(g)], indicating a strong interaction between polymer chains and hybrid nanofillers.

Large sized 2D nanosheets can act as a unique substrate for the growth of smaller sized 2D nanosheets, and the deposition of small

sized 2D nanosheets on the surface of large sized 2D nanosheets also mitigates agglomerations of nanosheets in the polymer matrix as well as imparting the PNCs with multifunctional properties.<sup>29–32</sup> For instance, Qian and co-workers synthesized a layered double hydroxide (LDH)/MoS<sub>2</sub> hybrid by a simple solution-processed self-assembly.<sup>31</sup> Because effective physical and strong electronic coupling existed between 2D LDH and MoS<sub>2</sub>, negatively charged MoS<sub>2</sub> nanosheets will interact with LDH nanosheets when they are mixed ultrasonically to form the LDH/MoS<sub>2</sub> hybrid. The LDH are decorated on the surface of exfoliated MoS<sub>2</sub> nanosheets among the LDH/MoS<sub>2</sub> hybrid. After introducing the hybrid into the epoxy, the nanocomposite shows largely improved fire retardancy. The r-GO nanosheets have also been applied as the growth substrate for other 2D nanosheets. For instance, Hu and co-workers combined r-GO nanosheets with Ni-Fe LDH by *in situ* solvothermal routes.<sup>29</sup> The Ni-Fe LDH decorated on the surface of wrinkled r-GO nanosheets exhibits a loose lamellar structure, preventing the restacking of r-GO nanosheets effectively. With incorporation of the r-GO/LDH hybrid into the epoxy, the nanocomposite shows excellent flame retardant properties compared with neat epoxy.

## C. 2D-3D hybrid nanofillers

3D nanoparticles have attracted tremendous attention as nanofillers for PNCs because of their high surface area and various functions.<sup>33</sup> In addition, the 3D nanoparticles can be decorated on the surface of 2D nanosheets to form a 2D-3D hybrid solving poor dispersion and agglomeration of 2D nanosheets in the polymer matrix.<sup>14</sup>

Various nanoparticles have been hybridized with 2D nanofillers, thus enhancing the functionality of 2D nanofillers. For instance, magnetic nanoparticles have been incorporated with r-GO nanosheets to improve the electromagnetic wave absorption property. Among 3D magnetic hybrid nanofillers, Fe<sub>3</sub>O<sub>4</sub> have largely been focused due to their magnetic properties, low toxicity, and good biocompatibility. Gao and co-workers prepared a r-GO/Fe<sub>3</sub>O<sub>4</sub> hybrid with Fe<sub>3</sub>O<sub>4</sub> nanoparticles densely coated on the surface of r-GO via chemical approaches, and the hybrid shows superparamagnetic and conductive properties.<sup>34</sup> The size and coverage of nanoparticles on 2D r-GO nanosheets show large influences on the final magnetic performance of PNCs. Due to fine dispersion of as-prepared r-GO/Fe<sub>3</sub>O<sub>4</sub> hybrid, highly flexible and multifunctional nanocomposites composed of polyurethane elastomer and r-GO/Fe<sub>3</sub>O<sub>4</sub> hybrid are fabricated by solution-blending. 3D Co<sub>3</sub>O<sub>4</sub>, as a semiconductor, has been extensively investigated in many areas due to its nontoxicity and low cost. Cao and co-workers fabricated a r-GO/Co<sub>3</sub>O<sub>4</sub> hybrid by *in situ* growth of Co<sub>3</sub>O<sub>4</sub> under mild wet-chemical conditions.<sup>10</sup> Unique core-shell nanostructures are formed with uniform-sized Co<sub>3</sub>O<sub>4</sub> nanoparticles embedded in r-GO layers. Moreover, the r-GO/Co<sub>3</sub>O<sub>4</sub>/poly(vinylidene fluoride) nanocomposite possesses excellent microwave-absorption properties. Two kinds of dimension-different nanofillers will show a unique “filler to filler” interaction in the polymer matrix; for instance, nanoplate-like clay and nanoglobe-like silica (SiO<sub>2</sub>) can be well dispersed in a poly(phenylene sulfide) (PPS) matrix via melt compounding.<sup>35</sup> The hybridization of SiO<sub>2</sub> nanoparticles with MoS<sub>2</sub> nanosheets will form core-shelled hybrid nanofillers, largely

showing enhancements in anticorrosive and mechanical performance of epoxy nanocomposites.<sup>36</sup> The hybrid of MoS<sub>2</sub> nanosheets and SiO<sub>2</sub> nanospheres can also be introduced into the polyacrylonitrile (PAN) spinning solution to construct the PAN/MoS<sub>2</sub>/SiO<sub>2</sub> composite fibers with excellent mechanical, thermal, and flame-retardant properties.<sup>37</sup>

The hybridization of conjugated polymer nanoparticles and r-GO has been expanded for electric device and luminescent applications. Among conjugated polymers, polypyrrole (PPy) has attracted enormous attention due to its good electrical conductivity, environmental stability, facile synthesis, easy processability, and low cost. Nosheen and co-workers synthesized the r-GO/PPy/epoxy nanocomposites by mixing PPy with r-GO followed by being incorporated into the epoxy matrix.<sup>38</sup> The r-GO/PPy/epoxy nanocomposites exhibit considerable enhancements in both mechanical and thermal performance compared with neat epoxy. Sharif and co-workers fabricated epoxy nanocomposites with GO/PPy hybrid nanofillers via *in situ* chemical polymerization.<sup>39</sup> The PPy nanoparticles were uniformly dispersed on the GO surface. The electrical, thermal, and mechanical properties of the GO/PPy hybrid outperform that of neat GO and PPy, confirming a synergistic effect of the GO/PPy hybrid as a multifunctional nanofiller.

### III. CONCLUSIONS AND PERSPECTIVE

In summary, a “hybridization” functionalization strategy for the construction of hybrid nanofillers containing 2D nanosheets is highlighted. Synergistic dispersion and function of hybrid nanofillers can be easily achieved due to homogeneous dispersion of hybrid nanofillers within the polymer matrix and strong interfacial interactions between hybrid nanofillers and the polymer matrix. Future research directions for the development of hybrid nanofillers for PNCs are also proposed. First, the evaluation of the dispersion state of hybrid nanofillers within the polymer matrix, as well as the nanofiller/matrix interfacial interaction, needs to be quantitative. In most cases, it is evident that the good dispersion and strong interfacial interaction are major indicators of these concerns. This is apparently right; however, the quantification of “good” and “strong” has not yet been quantitatively calibrated. Therefore, it is very meaningful to establish a more indexed relationship between the dispersion state, interfacial interaction, and final physical properties of PNCs. Second, to fulfill complex scopes of applications of PNCs, an integration rule for the rational design and controllable preparation of hybrid nanofillers for multifunctional PNCs is urgently demanded. For instance, in addition to enhancing the mechanical, thermal, and electrical properties of PNCs, the strain sensing, self-healing, and electromagnetic shielding performance are very important to be further incorporated into the PNCs. Third, the scale-up production of PNCs and their follow-up applications should be carefully considered. New-emerging fabricating methods or new-emerging 2D materials should be carefully focused for the development of scale-up production of PNCs. The value added applications of such new-emerging PNCs include flexible displays, electronic skins, and artificial muscles. To promote the fabrication and potential applications of PNCs with new-emerging hybrid nanofillers, the cooperation between researchers from various fields including materials science, physics, electronics, biology, and engineering is required.

### ACKNOWLEDGMENTS

We are grateful for the financial support from the National Natural Science Foundation of China (Grant No. 51773035), the National Science Foundation of Shanghai (Grant No. 17ZR1439900), the Fundamental Research Funds for the Central Universities and Graduate Student Innovation Fund of Donghua University (Grant No. CUSF-DH-D-2019026), and the Ministry of Education of the People’s Republic of China (Grant No. 6141A020033233).

### REFERENCES

- 1 J. N. Coleman, M. Lotya, A. O’Neill, S. D. Bergin, P. J. King, U. Khan, K. Young, A. Gaucher, S. De, R. J. Smith, I. V. Shvets, S. K. Arora, G. Stanton, H. Y. Kim, K. Lee, G. T. Kim, G. S. Duesberg, T. Hallam, J. J. Boland, J. J. Wang, J. F. Donegan, J. C. Grunlan, G. Moriarty, A. Shmeliov, R. J. Nicholls, J. M. Perkins, E. M. Grieveson, K. Theuwissen, D. W. McComb, P. D. Nellist, and V. Nicolosi, *Science* **331**(6017), 568–571 (2011).
- 2 K. E. Prasad, B. Das, U. Maitra, U. Ramamurty, and C. N. Rao, *Proc. Natl. Acad. Sci. U. S. A.* **106**(32), 13186–13189 (2009).
- 3 X. Liang and Q. Cheng, *Compos. Commun.* **10**, 122–128 (2018).
- 4 S. Sinha Ray and M. Okamoto, *Prog. Polym. Sci.* **28**(11), 1539–1641 (2003).
- 5 Z. Huang, L. Li, Y. Wang, C. Zhang, and T. X. Liu, *Compos. Commun.* **8**, 83–91 (2018).
- 6 O. Eksik, J. Gao, S. A. Shojaei, A. Thomas, P. Chow, S. F. Bartolucci, D. A. Lucca, and N. Koratkar, *ACS Nano* **8**(5), 5282–5289 (2014).
- 7 B. Radisavljevic, A. Radenovic, J. Brivio, V. Giacometti, and A. Kis, *Nat. Nanotechnol.* **6**(3), 147–150 (2011).
- 8 G. Kucinskis, G. Bajars, and J. Kleperis, *J. Power Sources* **240**, 66–79 (2013).
- 9 W. D. Zhang, I. Y. Phang, and T. X. Liu, *Adv. Mater.* **18**(1), 73–77 (2006).
- 10 G. Wang, Y. Wu, Y. Wei, X. Zhang, Y. Li, L. Li, B. Wen, P. Yin, L. Guo, and M. Cao, *ChemPlusChem* **79**(3), 375–381 (2014).
- 11 K. Q. Zhou, Y. X. Hu, J. J. Liu, Z. Gui, S. H. Jiang, and G. Tang, *Mater. Chem. Phys.* **178**, 1–5 (2016).
- 12 C. Zhang, S. Huang, W. W. Tjiu, W. Fan, and T. X. Liu, *J. Mater. Chem.* **22**(6), 2427–2434 (2012).
- 13 C. Zhang, W. W. Tjiu, W. Fan, Z. Yang, S. Huang, and T. X. Liu, *J. Mater. Chem.* **21**(44), 18011–18017 (2011).
- 14 Z. Huang, H. Guo, and C. Zhang, *Compos. Commun.* **12**, 117–122 (2019).
- 15 K. N. Wan, S. L. Liu, C. Zhang, L. Li, Z. Zhao, T. X. Liu, and Y. Xie, *ChemNanoMat* **3**(6), 447–453 (2017).
- 16 C. Tang, G. Long, X. Hu, K. W. Wong, W. M. Lau, M. Fan, J. Mei, T. Xu, B. Wang, and D. Hui, *Nanoscale* **6**(14), 7877–7888 (2014).
- 17 F. Zhang, Y. Y. Feng, M. M. Qin, T. X. Ji, F. Lv, Z. Y. Li, L. Gao, P. Long, F. L. Zhao, and W. Feng, *Carbon* **145**, 378–388 (2019).
- 18 B. Pradhan and S. K. Srivastava, *Polym. Int.* **63**(7), 1219–1228 (2014).
- 19 R. Andrews, D. Jacques, D. Qian, and T. Rantell, *Acc. Chem. Res.* **35**(12), 1008–1017 (2002).
- 20 C. Zhang, W. W. Tjiu, T. Liu, W. Y. Lui, I. Y. Phang, and W. D. Zhang, *J. Phys. Chem. B* **115**(13), 3392–3399 (2011).
- 21 K. Zhou, J. Liu, Y. Shi, S. Jiang, D. Wang, Y. Hu, and Z. Gui, *ACS Appl. Mater. Interfaces* **7**(11), 6070–6081 (2015).
- 22 S. Li, H. Qin, T. Zhang, H. P. Cong, and S. H. Yu, *Small* **14**(22), 1800673 (2018).
- 23 N. Bunekar, T.-Y. Tsai, and H.-P. Huang, *Polym.-Plast. Technol. Mater.* **58**(5), 547–559 (2018).
- 24 S. Das, H. Y. Chen, A. V. Penumatcha, and J. Appenzeller, *Nano Lett.* **13**(1), 100–105 (2013).
- 25 X. Wang, P. Wang, J. Wang, W. Hu, X. Zhou, N. Guo, H. Huang, S. Sun, H. Shen, T. Lin, M. Tang, L. Liao, A. Jiang, J. Sun, X. Meng, X. Chen, W. Lu, and J. Chu, *Adv. Mater.* **27**(42), 6575–6581 (2015).
- 26 L. Najafi, B. Taheri, B. Martin-Garcia, S. Bellani, D. Di Girolamo, A. Agresti, R. Oropesa-Nunez, S. Pescetelli, L. Vesce, E. Calabro, M. Prato, A. E. Del Rio Castillo, A. Di Carlo, and F. Bonaccorso, *ACS Nano* **12**(11), 10736–10754 (2018).

- <sup>27</sup>T. Pham, G. Li, E. Bekyarova, M. E. Itkis, and A. Mulchandani, *ACS Nano* **13**(3), 3196–3205 (2019).
- <sup>28</sup>H. Ribeiro, J. P. C. Trigueiro, W. M. Silva, C. F. Woellner, P. S. Owuor, A. Cristian Chipara, M. C. Lopes, C. S. Tiwary, J. J. Pedrotti, R. Villegas Salvatierra, J. M. Tour, N. Chopra, I. N. Odeh, G. G. Silva, and P. M. Ajayan, *ACS Appl. Mater. Interfaces* **11**(27), 24485–24492 (2019).
- <sup>29</sup>X. Wang, S. Zhou, W. Xing, B. Yu, X. Feng, L. Song, and Y. J. Hu, *J. Mater. Chem. A* **1**(13), 4383–4390 (2013).
- <sup>30</sup>R. Gao, S. Wang, K. Zhou, and X. Qian, *Polym. Adv. Technol.* **30**(4), 879–888 (2019).
- <sup>31</sup>K. Zhou, R. Gao, and X. Qian, *J. Hazard. Mater.* **338**, 343–355 (2017).
- <sup>32</sup>P. Zhang, C. Shao, Z. Zhang, M. Zhang, J. Mu, Z. Guo, Y. Sun, and Y. Liu, *J. Mater. Chem.* **21**(44), 17746–17753 (2011).
- <sup>33</sup>J. Njuguna, K. Pielichowski, and S. Desai, *Polym. Adv. Technol.* **19**(8), 947–959 (2008).
- <sup>34</sup>H. He and C. Gao, *ACS Appl. Mater. Interfaces* **2**(11), 3201–3210 (2010).
- <sup>35</sup>Y. Yang, H. Duan, S. Zhang, P. Niu, G. Zhang, S. Long, X. Wang, and J. Yang, *Compos. Sci. Technol.* **75**, 28–34 (2013).
- <sup>36</sup>Y. Xia, Y. He, C. Chen, Y. Wu, and J. Chen, *Prog. Org. Coat.* **132**, 316–327 (2019).
- <sup>37</sup>H. Peng, D. Wang, M. Li, L. Zhang, M. Liu, and S. Fu, *Compos. Part B-Eng.* (2019).
- <sup>38</sup>S. Nosheen, M. A. Raza, S. Alam, M. Irfan, A. Iftikhar, F. Iftikhar, B. Waseem, Z. Abbas, and B. Soomro, *Arabian J. Sci. Eng.* **42**(1), 193–199 (2017).
- <sup>39</sup>R. Moosaei, M. Sharif, and A. Ramezannezhad, *Polym. Test.* **60**, 173–186 (2017).